Engineering Structures 33 (2011) 1742–1753

Contents lists available at ScienceDirect

Engineering Structures

journal homepage: www.elsevier.com/locate/engstruct

Prediction of punching shear strength of two-way slabs

Ahmed A. Elshafey [a,b,*], Emad Rizk [c], H. Marzouk [d], Mahmoud R. Haddara [c]

[a] Faculty of Engineering, Minufiya University, Egypt
[b] Memorial University of Newfoundland, Canada
[c] Faculty of Engineering and Applied Science, Memorial University of Newfoundland, St. John's, Newfoundland, Canada
[d] Faculty of Engineering, Architecture and Science, Ryerson University, Toronto, Ontario, Canada

ARTICLE INFO

Article history:
Received 30 July 2010
Received in revised form
24 December 2010
Accepted 15 February 2011
Available online 17 March 2011

Keywords:
Concrete strength
Reinforcement ratio
Size effect
Neural networks
Punching shear strength

ABSTRACT

The punching shear strength of two way slabs without shear reinforcement and without unbalanced moment transfer is estimated using both neural networks and new simplified punching shear equations. An artificial neural network (ANN) was used to predict the punching shear strength of internal slab–column connections. Neural network analysis is conducted using 244 test data available in the literature and experiments conducted by the authors to evaluate the influence of concrete strength, reinforcement ratio and slab effective depth on punching shear strength. A wide range of slab thicknesses (up to 500 mm) and reinforcement ratios were used. In general, the results obtained from the neural network are very close to the experimental data available. The test results were used to develop two new simplified practical punching shear equations. The equations also showed a very good match with available experimental data. Four equations for the punching shear strength prescribed in well-known specifications were evaluated based on the available experimental results. This paper includes a discussion of the parameters of punching shear strength in the American, Canadian, British and European specifications.

© 2011 Elsevier Ltd. All rights reserved.

1. Introduction

The punching shear equations in the current building codes are empirical in nature. These equations are based on the statistical fitting of test results available at the time of developing these equations. Several equations have been proposed to predict the punching shear capacity of concrete slabs. The two equations that are used in North America are the ACI 318-08 [1] and CSA-A23.3-04 [2] equations. In Europe, the BS 8110-97 [3], CEB-FIP-90 [4] and Euro-code 2 (2004) [5] are among the most common codes. North American and European equations differ with regards to the calculation of shear strength and the ways that the shear strength is converted into a loading capacity.

The main objectives of the present study are to use test results available in the open literature to introduce reliable and accurate practical methods for punching shear calculations for both thin and thick slabs. Two methods for fitting the experimental results are used: a neural network fit and regression analysis. A neural network is used to find the best fit for test results of 244 slabs available in the literature. The neural network predictions were very close to the test results and provided a very good tool for punching shear calculations. The neural network was trained using a 60% of the available testing data. Very accurate estimates were obtained for the punching shear load. A number of parameters were easily accounted for the neural network.

Regression analysis was used to obtain explicit equations for the shear punching load. The proposed equations gave excellent estimates for the shear punching load. The database used included test results for a wide range of slab thicknesses and reinforcement ratios. Both neural networks and the proposed equations provide the designer with a reliable tool to for estimating punching shear strength of two way concrete slabs. The tool is based on the use of large number of data sets, which provide a wider application. The work done before was based on thin slabs and was applied for both thin and thick slabs. Publications on the use of neural networks in predicting shear strength are very few. The data which was available to train the network included a limited range of slab thicknesses (35–120 mm). By considering the available up to date experimental data, the estimation of the punching shear is improved and can be applied to slab thicknesses up to 500 mm.

* Corresponding author at: Faculty of Engineering, Minufiya University, Egypt. Tel.: +1 709 7378208.
E-mail address: aelshafey@mun.ca (A.A. Elshafey).

0141-0296/$ – see front matter © 2011 Elsevier Ltd. All rights reserved.
doi:10.1016/j.engstruct.2011.02.013

Nomenclature

A_o	The area of the critical section surface
a_{crit}	Distance from the column face to the control perimeter
C	Column side dimension
$C_{RD,C}$	Factor depending on γ_c
d	Effective depth to the center of the tensile reinforcement
E	Modulus of elasticity
$\acute{f}_c$	Uniaxial compressive strength of concrete (cylinder strength)
f_{ck}	Characteristic compressive strength of the concrete in MPa
f_{ct}	Tensile strength of concrete
f_y	Yield stress of steel reinforcement
G_f	Fracture energy
h	Slab height
k	Size factor of the effective depth
l_{ch}	Characteristic length of concrete material based on fracture mechanics
P	Punching shear capacity
$v_{\min}$	Minimum shear capacity of the concrete
$v_{RD,C}$	Punching shear stress resistance in accordance to the Euro-code 2 (2004)
v_c	Nominal shear strength (or nominal shear/unit length) provided by the concrete
γ_c	Material resistance factor of concrete
λ	Modification factor of lightweight concrete
ρ	Ratio of flexure reinforcement %
μ	The mean value
σ	Standard deviation

2. Literature survey

Examples of the use of artificial neural networks in the area of concrete structures can be found in the literature. Bhatt and Agar [6] applied a radial bases ANN for the prediction of the ultimate punching load in the case of an internal flat slab–column junction with no shear reinforcement. Over 150 test data that covers slab thickness range from 35 mm up to 120 mm. Neural network prediction was found to give better results compared with the British code BS8110-97. An artificial neural network was used to predict the strength and slump of ready mix concrete and high strength concrete, in which chemical admixtures and/or mineral additives were used [7]. The concrete's strength at different ages was estimated using a neural network to determine appropriate times for form removal [8]. The evaluation of concrete slabs' performance of existing bridges was performed using a neural network [9]. A neural network was used to predict the shear capacity of anchor bolts located near a concrete edge [10]. Hoła and Schabowicz [11] used a non-destructive technique and a neural network approach to evaluate the strength of concrete. Neural networks were used to optimize the cost of the design of reinforced concrete slabs [12]. A neural network approach was used to develop a methodology for a concrete mix which has lower cement and water contents, higher durability, better economical and ecological effects [13]. Öztaş et al. [14] used a neural network approach to predict the concrete's compressive strength and the slump value. Choi et al. [15] proposed an alternative approach for predicting the punching shear strength of concentrically loaded interior slab–column connections using fuzzy logic. A total of 178 experimental datasets from the literature were used in training and testing the fuzzy logic system. It was noted that the fuzzy logic-based model improved the predictions of the punching shear strength of concentrically loaded interior slab–column connections. Neural networks have been used to predict the inelastic moments in continuous composite beams considering instantaneous cracking, shrinkage, and creep effects [16].

Demir [17] used an artificial neural network to predict the elastic moduli of both normal and high strength concrete. A neural network model was successfully used to determine the 3D response of the fundamental periods, maximum values of base shear-forces, base bending moments and top-floor displacement time histories for buildings [18]. Trtnik et al. [19] used ultrasonic pulse velocity and a neural network approach to predict the concrete's strength. Neural networks were used to predict the compressive strength of lightweight concrete mixtures at different ages of curing [20]. Neural networks were used to determine the shear strength of circular reinforced concrete columns, the results obtained agreed with the results obtained using various codes [21]. An artificial neural network was proposed for modeling the bond between conventional ribbed steel bars and concrete [22]. Erdem [23] applied artificial neural networks to predict the ultimate moment capacity of reinforced concrete slabs in fires. The back-propagation neural network was applied for an analytical model to predict the structural capacity of a stub-girder system [24].

3. Design codes for two-way slabs

Most design codes use the critical section (control perimeter) approach in the design of a slab–column connection for a two-way slab. According to this method, the nominal shear stress caused by gravity loads is determined at an assumed vertical critical section around the column. The shear stress should be limited to a nominal design value, which is usually assumed to be a function of concrete's strength and the geometric parameters of the slab and column. This method is simple and leads to reasonable estimates if properly formulated.

Different codes define considerably different dimensions and shapes of the critical section. This results in different associated nominal shear strength. Codes also differ in the choice of parameters that affect the connection punching strength. Marzouk and Hussein [25] and Gardner [26] recommended the use of the cubic root, where the shear stress is proportional to the cubic root of the concrete's compressive strength, as a better option than the use of the square root for high strength concrete specimens with concrete strength more than 40 MPa. The analysis of the present results is made in relation to ACI 318-08; BS8110-97; CEB-FIP-90 and Euro-code 2 (2004) codes.

3.1. ACI 318-08

In the Building Code of ACI 318-08, a simple equation is applied for the design. The equation is developed based on the classical shear strength equation. In ACI 318-08, the control perimeter is only $0.5d$ from the loaded area. The ACI code has no influence from either the main steel ratio or the effective depth of the slab in its limiting shear stress. ACI 318-08 requires that the ultimate shear resistance for slabs without shear reinforcement, v_c, be approximated by using the following expression:

$$v_c = 0.33\lambda\sqrt{\acute{f}_c} \quad \text{(MPa)} \tag{1}$$

Table 1
Analytical results.

Equation	Mean (μ)	Standard deviation (σ)	Coefficient of variation (%)	95% confidence interval
$V_{test}/V_{CSA-A23.3-04}$	1.25	0.34	27.20	1.25 ± 0.043
$V_{test}/V_{ACI-318-08}$	1.09	0.29	26.60	1.09 ± 0.036
$V_{test}/V_{CEB-FIB-90}$	0.95	0.13	13.68	0.95 ± 0.016
$V_{test}/V_{BS8110-97}$	1.02	0.13	12.75	1.02 ± 0.016
$V_{test}/V_{EC2(2004)}$	1.16	0.21	18.10	1.16 ± 0.026
V_{test}/V_{neural}	0.92	0.17	18.48	0.92 ± 0.021
$V_{test}/V_{Eq.(8)}$	1.00	0.15	15.00	1.00 ± 0.019
$P_{test}/P_{Eq.(9)}$	1.00	0.12	12.00	1.00 ± 0.015

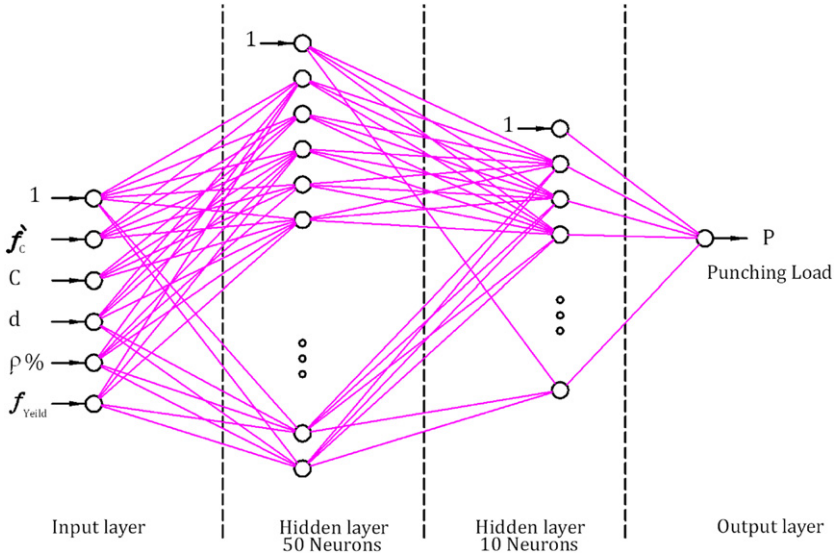

Fig. 1. Neural network architecture.

where λ is the modification factor reflecting the reduced mechanical properties of lightweight concrete (λ = 1.0 for normal-weight concrete, 0.85 for sand-lightweight concrete, and 0.75 for all-lightweight concrete), and $\hat{f}_c$ is the cylinder compressive strength of concrete, MPa. The Canadian Code CSA-A23.3-04 expression accounts for the slab's effective depth. If the effective depth, d, used in two-way shear calculations exceeds 300 mm, the value of v_c shall be multiplied by $1300/(1000 + d)$. Fracture mechanics concepts suggest that the size effect factor is not only related to the member's depth but also can be related to the concrete's mechanical properties as well.

3.2. European codes

Modern European codes in practice, treat punching in terms of shear stresses calculated for control perimeters at relatively large distances from columns or loaded areas. According to the CEB-FIP-90 and Euro-code 2 (2004) equations, the distance is $2d$. In BS 8110-97, it is $1.5d$, but the perimeter has square corners in comparison to the rounded corners of the CEB-FIP-90 model code.

3.3. CEB-FIP-90

The CEB-FIB 90 code recommends that the punching shear resistance, v_{CEB}, is expressed as proportional to $(f_{ck})1/3$, where f_{ck} is the characteristic compressive strength of concrete, MPa. The highest concrete grade considered in the CEB-FIP-90 code is C80, which corresponds to f_{ck} is equal to 80 MPa. Influences of reinforcement and slab depth are also considered in this design code. The relevant characteristic resistance in accordance to the CEB-FIP-90 code is:

$$v_{CEB} = 0.18k\,(100\rho f_{ck})^{1/3} \quad \text{(MPa)} \tag{2}$$

where $k = 1 + (200/d)1/2$ is a size-effect coefficient, d is the slab effective depth, mm, and ρ is the ratio of flexure reinforcement. The length of the control perimeter is calculated at a distance equal to $2d$ from the column face.

3.4. Euro-code 2 (2004)

The Euro-code 2 (2004) code recommends that the punching shear resistance, $V_{RD,C}$ is expressed as proportional to $(f_{ck})^{1/3}$, where f_{ck} is the characteristic compressive strength of concrete, MPa. Influences of reinforcement and slab depth are also considered in this design code. The punching shear stress resistance in accordance to the Euro-code 2 (2004) code is calculated as:

$$v_{RD,C} = C_{RD,C}k\,(1000\rho f_{ck})^{1/3}\frac{2d}{a_{crit}} \geq v_{min}\frac{2d}{a_{crit}} \quad \text{(MPa)} \tag{3}$$

where $C_{Rd,c} = 0.18/\gamma_c$ is an empirical factor derived from a regression analysis, with γ_c being the material resistance factor for concrete (=1.5); d is the effective depth, mm; $k = 1 + \sqrt{200/d} \leq 2.0$ is the size factor of the effective depth; ρ is the flexural reinforcement ratio ≤2%; f_{ck} is the characteristic cylinder compressive concrete strength, MPa; a_{crit} is the distance from the column face to the control perimeter considered, mm. The minimum shear capacity of the concrete, including the material resistance factor for concrete $\gamma_c = 1.5$ is given by:

$$v_{min} = 0.035k^{3/2}\sqrt{f_{ck}} \quad \text{(MPa)}. \tag{4}$$

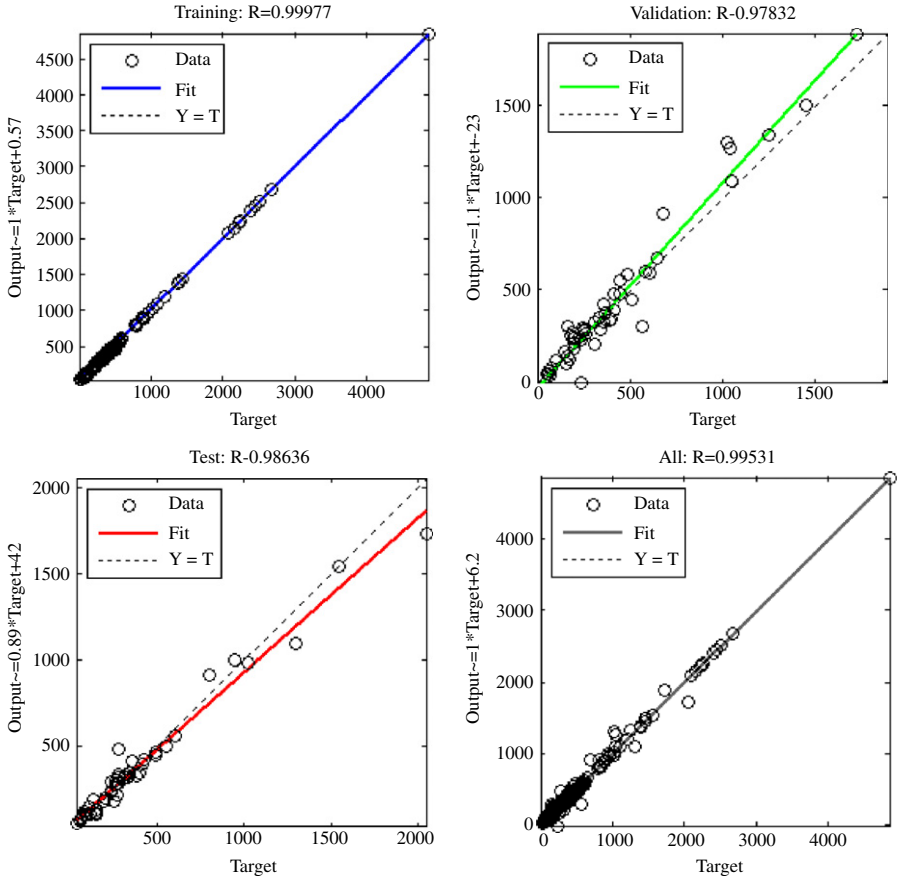

Fig. 2. Regression during training process.

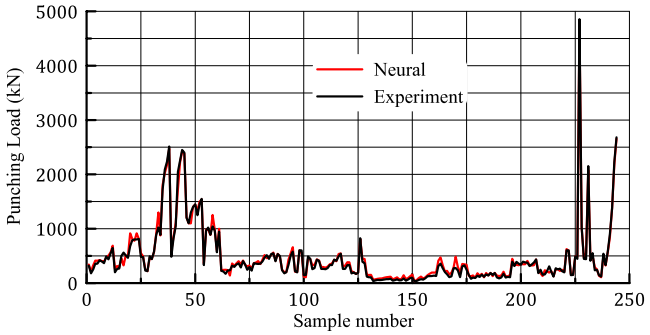

Fig. 3. Experimental and predicted concrete strength.

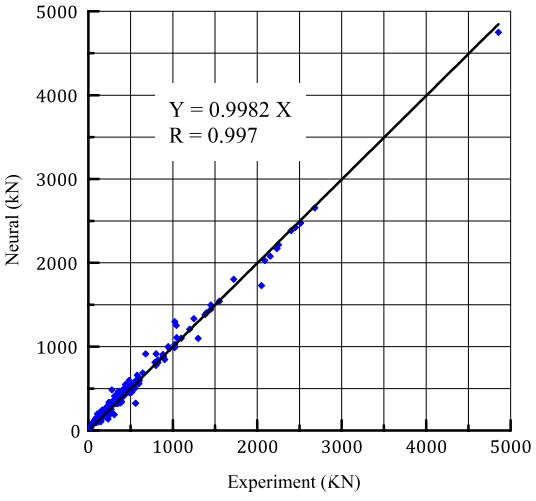

Fig. 4. Experimental and predicted concrete strength.

3.5. BS 8110-97

The punching shear stress resistance in accordance to BS 8110-97 is:

$$v_{BS} = 0.79\left(100\rho\frac{\grave{f}_c/0.78}{25}\right)^{1/3}\left(\frac{400}{d}\right)^{1/4} \quad \text{(MPa)} \tag{5}$$

where $(400/d)^{1/4}$ is a size-effect coefficient, the critical perimeter for both circular and square loaded areas being the length of a square perimeter $1.5d$ from the loaded area, d is the slab's effective depth, mm, and ρ is the ratio of flexure reinforcement.

4. Punching shear database

A total of 244 experimental data on interior slab–column connections subjected to symmetrical punching were collected and reviewed. The database is presented in the Appendix, Tables A.1–A.7. All specimens were reinforced concrete slab–column connections without drop panels, column capitals, or any type of shear reinforcement. Specimens cast with lightweight concrete were excluded. The collected experimental results are available in the literature and were conducted by different researchers [27–36,26,37,25,38–47]. The concrete's compressive strength, $\acute{f}_c$, for the analyzed database ranges from 13 to 120 MPa, the ratio of flexure reinforcement, ρ, ranges from 0.25% to 5% while the slab's effective depth, d, for the analyzed database ranges from 35 to 500 mm. The objective is to study the influence of concrete strength, reinforce-

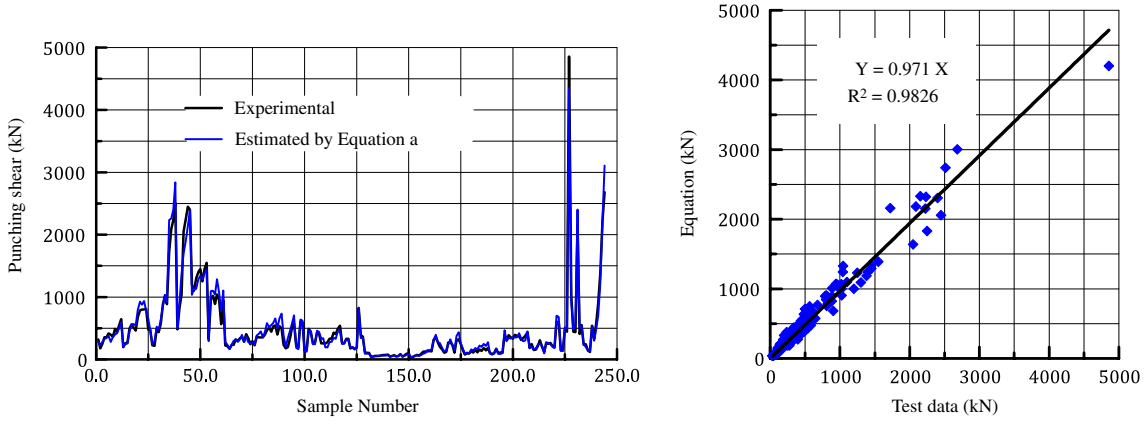

(a) Proposed equation versus sample number. (b) V_{test} vs. $V_{equation\ a}$.

Fig. 5. Comparison of proposed Equation a with the Experimental results.

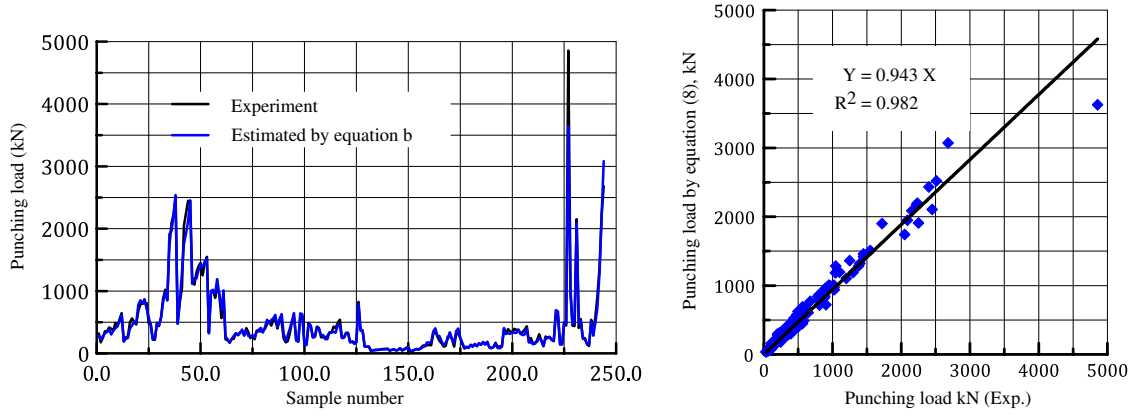

(a) Proposed equation b versus sample number. (b) V_{test} versus $V_{equation\ b}$.

Fig. 6. Comparison of proposed Equation b with the selected database results.

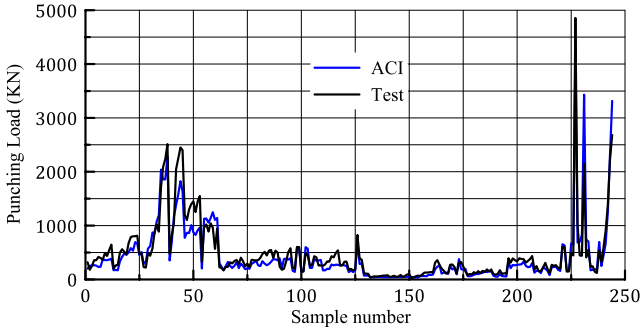

Fig. 7. ACI 318-08 equation versus test results.

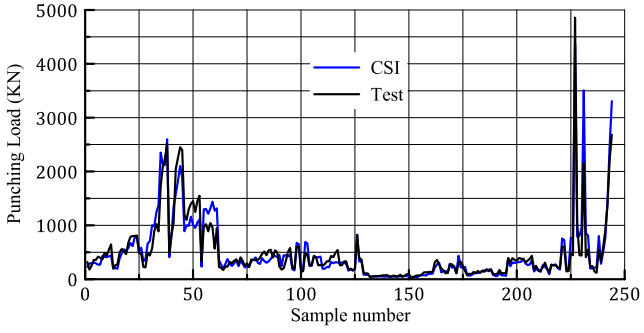

Fig. 8. CSA-A23.3-04 equation versus test results.

ment ratio and slab effective depth (size effect) on punching shear capacity. In the current study the punching shear strength was calculated for a control perimeter at 0.5d, 1.5d and 2.0d distance from the column face. This is the same control perimeter used by ACI 318-08, BS8110-97, CEB-FIP-90 and Euro-code 2 (2004), respectively.

5. Size effect

For design engineers, the size effect is a useful concept that is based on fracture mechanics. The size of the fracture process zone is represented by a material property called the characteristic length, l_{ch}. It expresses the fracture properties of the concrete, such as the modulus of elasticity, E_c, the fracture energy, G_f and the tensile strength, f_{ct}, where f_{ct} is the direct tensile strength of concrete as determined by the direct tension test [48] or any other fracture mechanics test:

$$l_{ch} = \frac{E_c G_f}{f_{ct}^2} \tag{6}$$

G_f is defined as the amount of energy required to cause one unit area of a crack, it can be obtained as the area under the "load-crack width curve". However, the characteristic length has no physical correspondence, i.e., it is not a real length that can be measured. A higher value of l_{ch} reflects that the material is less brittle and a smaller value means that the material is more brittle. In an earlier investigation by Marzouk and Chen [48],

Table A.1
Slab-column connections with circular/square columns under symmetrical punching.

ID	Col. type	h, mm	C, mm	d, mm	ρ%	V_{test}, kN	f'_c, MPa	f_y, MPa	V_{test}/V_{code}						Ref.
									ACI 318-08	CEB-FIP-90	BS8110-97	EC 2 (2004)	Eq. (8)	Eq. (9)	
A-1b	S	152	254	118	1.16	365	25.2	332	1.25	1.04	0.98	1.13	0.97	1.02	
A-1c	S	152	254	118	1.16	356	29.0	332	1.14	0.97	0.91	1.05	0.90	0.94	
A1-d	S	152	254	118	1.16	351	36.8	332	1.00	0.88	0.83	0.96	0.80	0.86	
A-1e	S	152	254	118	1.16	356	20.3	332	1.36	1.09	1.03	1.18	1.04	1.07	
A2-b	S	152	254	114	2.50	400	19.5	321	1.64	1.01	0.95	1.10	0.92	0.93	
A-2c	S	152	254	114	2.50	467	37.4	321	1.38	0.95	0.89	1.04	0.83	0.87	
A-7b	S	152	254	114	2.50	512	27.9	321	1.75	1.14	1.08	1.26	1.02	1.06	
A-3b	S	152	254	114	3.74	445	22.6	321	1.69	0.93	0.88	1.02	0.83	0.84	
A-3c	S	152	254	114	3.74	534	26.5	321	1.87	1.06	1.00	1.17	0.94	0.95	
A-3d	S	152	254	114	3.74	547	34.5	321	1.68	1.00	0.94	1.10	0.86	0.89	[27]
A-4	S	152	356	118	1.18	400	26.1	332	1.06	0.96	0.91	1.05	0.82	0.96	
A-5	S	152	356	114	2.50	534	27.8	321	1.43	1.02	0.97	1.12	0.84	0.97	
A-6	S	152	356	114	3.74	498	25.0	321	1.41	0.86	0.82	0.95	0.70	0.80	
A-13	S	152	356	121	0.55	236	26.2	294	0.61	0.70	0.67	0.76	0.62	0.74	
B-1	S	152	254	114	0.48	178	14.2	324	0.85	0.86	0.81	0.94	0.87	0.91	
B-2	S	152	254	114	0.48	200	47.6	321	0.52	0.65	0.61	0.71	0.60	0.68	
B-4	S	152	254	114	1.01	334	47.7	303	0.87	0.84	0.80	0.93	0.76	0.83	
B-9	S	152	254	114	2.00	505	43.9	341	1.38	1.05	0.99	1.15	0.91	0.98	
B -14	S	152	254	114	3.02	578	50.5	325	1.47	1.00	0.94	1.10	0.85	0.90	
5	C	150	150	117	0.80	255	26.8	441	1.19	0.98	0.92	1.06	1.07	0.97	
6	C	150	150	118	0.79	275	26.2	454	1.29	1.06	0.99	1.14	1.16	1.05	
24	C	150	300	128	1.01	430	26.4	455	1.16	1.05	1.00	1.12	0.96	1.05	
25	C	150	300	124	1.04	408	25.1	451	1.17	1.05	1.00	1.13	0.95	1.04	
32	C	150	300	123	0.49	258	26.3	448	0.73	0.85	0.80	0.91	0.79	0.89	
33	C	150	300	125	0.48	258	26.6	462	0.71	0.83	0.79	0.89	0.78	0.88	
IA15a-5	C	150	106	117	0.80	255	23.6	441	1.52	1.12	1.05	1.21	1.35	1.12	
IA15a-6	C	150	106	118	0.79	275	23.0	454	1.64	1.21	1.13	1.30	1.46	1.21	
IA15c-11	C	150	106	121	1.53	333	28.8	436	1.71	1.05	0.99	1.13	1.21	1.00	[28]
IA15c-12	C	150	106	122	1.54	331	27.7	439	1.71	1.04	0.98	1.12	1.21	0.99	
IA30a-24	C	150	212	128	1.01	430	23.2	455	1.55	1.26	1.19	1.34	1.27	1.24	
IA30a-25	C	150	212	124	1.04	408	21.9	451	1.59	1.26	1.19	1.35	1.27	1.24	
IA30C-30	C	150	212	120	2.16	490	26.8	434	1.80	1.17	1.10	1.26	1.11	1.08	
IA30C-31	C	150	212	119	2.18	539	26.8	448	2.00	1.30	1.22	1.40	1.23	1.20	
IA30d-32	C	150	212	123	0.49	258	23.1	448	0.99	1.02	0.96	1.09	1.06	1.05	
IA30d-33	C	150	212	125	0.48	258	23.4	461	0.96	1.00	0.94	1.07	1.04	1.03	
IA30e-34	C	150	212	120	1.00	331	24.2	460	1.28	1.05	0.99	1.14	1.05	1.03	
IA30e-35	C	150	212	122	0.98	331	21.8	458	1.32	1.07	1.01	1.15	1.08	1.05	

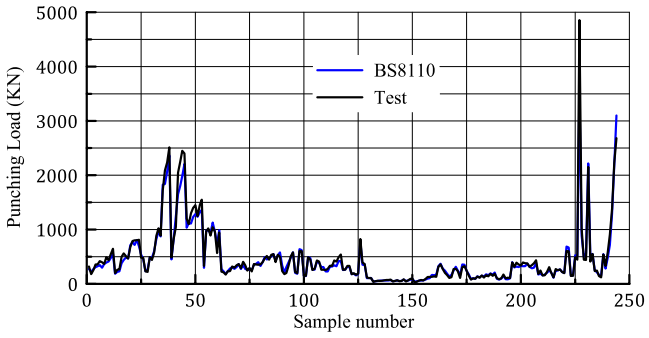

Fig. 9. BS 8110-97 equation versus test results.

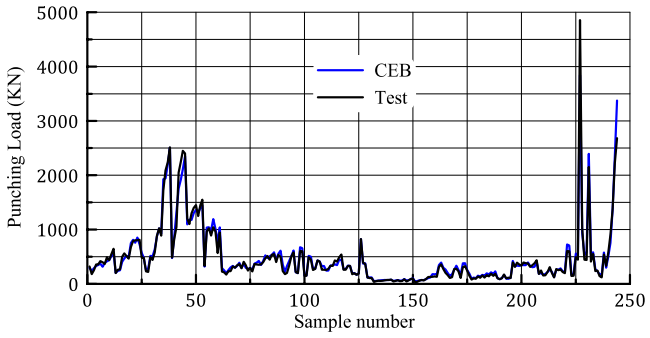

Fig. 10. CEB-FIP-90 equation versus test results.

the fracture energy, G_f, was determined experimentally for high-strength concrete to be 160 N/m compared to 110 N/m for normal strength concrete. These values have been estimated according to the results of the direct tension test. The fracture energy is calculated as the area under the descending portion of the stress-crack width curve. The characteristic length, l_{ch} was estimated to have an average value of 500 mm and 250 mm for normal and high-strength concrete, respectively. In this research, the term $(250/d)^{\alpha}$ was chosen to account for the size effect. The exponent, α, represents a sensitivity number. Based on the results of a finite element parametric study of 81 slabs by Marzouk et al. [49], it was found that the shear strength decreases as the brittleness of the concrete slab, h/l_{ch}, increases, where h is the slab thickness. The researchers recommended that the expression for shear strength to be rewritten for high-strength concrete application as follows:

$$v_u = 0.88 f_{ct} \left(\frac{C}{d}\right)^{-0.4} \sqrt[3]{\rho \left(\frac{l_{ch}}{h}\right)} \quad \text{(MPa)} \tag{7}$$

where C is the length of a side of a square column, mm, d is the effective depth of slab, mm, f_{ct} is the direct tensile strength of concrete, MPa, and ρ is the flexural reinforcement ratio. The brittleness ratio is not only a reflection of the size factor, but also a function of the tension and crack width relationship, concrete strength, and types of aggregate. The use of the brittleness ratio h/l_{ch} is much more meaningful than an empirical size factor. A

Table A.2
Slab-column connections with circular/square columns under symmetrical punching.

ID	Col. type	h, mm	C, mm	d, mm	ρ%	V_{test}, kN	f'_c, MPa	f_y, MPa	V_{test}/V_{code}						Ref.
									ACI 318-08	CEB-FIP-90	BS8110-97	EC 2 (2004)	Eq. (8)	Eq. (9)	
R-1	S	152	305	114	1.38	394	27.5	400	1.19	0.99	0.94	1.09	0.87	0.97	[29]
R-2	S	152	152	114	1.38	312	26.5	400	1.51	1.04	0.97	1.13	1.10	0.99	
S1-60	S	152	254	114	1.06	390	23.2	400	1.46	1.22	1.16	1.34	1.16	1.21	
S2-60	S	152	254	114	1.03	356	22.0	400	1.37	1.15	1.09	1.26	1.09	1.14	
S3-60	S	152	254	114	1.13	334	23.8	400	1.23	1.02	0.96	1.12	0.96	1.00	
S1-70	S	152	254	114	1.06	393	24.4	400	1.43	1.21	1.15	1.33	1.14	1.20	
S2-70	S	152	254	114	1.02	379	25.3	400	1.35	1.17	1.11	1.28	1.10	1.16	
S4-70	S	152	254	114	1.13	374	35.1	400	1.14	1.00	0.95	1.10	0.92	0.98	
S4A-70	S	152	254	114	1.13	312	20.4	400	1.24	1.00	0.94	1.10	0.95	0.98	
S5-60	S	152	203	114	1.06	343	22.1	400	1.52	1.20	1.13	1.31	1.20	1.17	
S5-70	S	152	203	114	1.06	379	24.2	400	1.61	1.28	1.21	1.40	1.28	1.25	
M1A	S	152	305	114	1.5	433	23.0	400	1.43	1.12	1.06	1.23	1.00	1.09	
1	C	102	221	82	1.21	182	13.9	457	1.48	1.05	0.98	1.26	1.03	1.05	[30]
II-4a	C	102	221	82	0.89	245	23.8	559	1.53	1.32	1.23	1.58	1.25	1.34	
II-5	C	102	221	82	0.53	152	22.8	471	0.97	0.99	0.92	1.18	0.96	1.04	
II-6	C	102	221	82	1.33	157	12.3	456	1.36	0.92	0.86	1.10	0.90	0.91	
II-8	C	102	333	82	0.59	219	24.8	456	0.98	1.08	1.01	1.29	0.94	1.18	
IIR20-2	C	129	201	109	0.93	307	19.8	500	1.56	1.25	1.18	1.39	1.28	1.24	
III-3	C	102	221	82	1.21	201	24.0	491	1.25	0.98	0.91	1.16	0.91	0.97	
7	C	102	119	82	0.74	118	13.2	456	1.48	1.05	0.97	1.24	1.23	1.05	
M3-1-0	S	70	152	51	1.10	79	21.1	386	1.27	0.91	0.83	1.23	0.90	0.92	[31]
M3-l-0a	S	70	152	51	2.20	99	18.0	336	1.72	0.96	0.87	1.29	0.93	0.92	
M-4-1-0	S	70	203	51	1.10	93	15.5	386	1.38	1.01	0.92	1.37	0.96	1.06	
M-4-2-0	S	70	203	50	2.20	133	27.2	386	1.51	0.97	0.88	1.31	0.85	0.96	
M-5-1-0	S	70	254	51	1.10	109	23.3	336	1.11	0.91	0.83	1.24	0.80	0.99	
M-5-2-0	S	70	254	51	2.20	152	22.9	386	1.55	1.02	0.92	1.38	0.86	1.05	
M-6-1-0	S	70	305	51	1.10	114	23.0	386	1.00	0.85	0.77	1.15	0.72	0.96	
M-6-2-0	S	70	305	50	2.20	159	26.4	386	1.31	0.91	0.83	1.24	0.73	0.97	
M-7-1-0	S	70	356	51	1.10	139	27.7	386	0.97	0.88	0.80	1.19	0.71	1.02	
M-7-2-0	S	70	356	51	2.20	184	25.0	386	1.35	0.96	0.87	1.30	0.75	1.06	
M-8-1-0	S	70	406	51	1.10	145	24.9	386	0.95	0.86	0.79	1.18	0.69	1.04	
M-8-2-0	S	70	406	50	2.20	185	24.6	386	1.23	0.89	0.81	1.21	0.68	1.01	
M-3-1-2	S	70	152	50	1.10	102	27.0	386	1.46	1.10	0.99	1.48	1.06	1.11	
M-2-1-0	S	70	102	50	1.10	86	28.5	386	1.59	1.09	0.98	1.46	1.17	1.06	
M-2-2-0	S	70	102	50	2.20	102	24.9	386	2.02	1.07	0.97	1.45	1.13	1.00	
M-3-l-0b	S	70	152	50	2.20	172	53.8	386	1.74	1.17	1.06	1.58	1.04	1.11	
M-3-l-4a	S	70	152	50	1.10	99	21.1	386	1.60	1.16	1.04	1.56	1.14	1.17	
M-3-l-4b	S	70	152	50	1.10	112	20.0	386	1.86	1.33	1.20	1.80	1.32	1.35	
M-3-2-4	S	70	152	50	2.20	105	17.0	386	1.90	1.05	0.95	1.42	1.02	1.01	

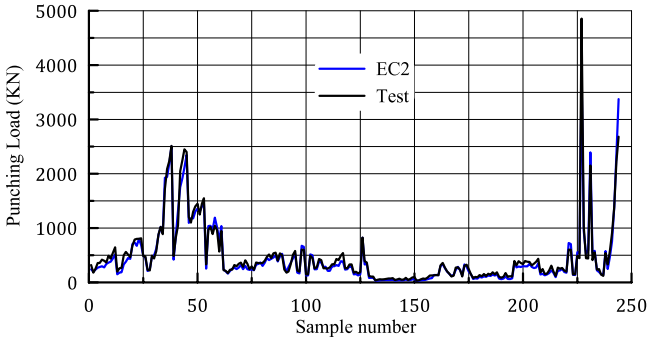

Fig. 11. EC2 (2004) equation versus test results.

similar expression was developed in Germany on punching shear capacity of point supported, reinforced concrete slabs by Staller [50].

6. Neural networks

The artificial neural network is a mathematical tool that attempts to imitate the working of biological neurons in a human brain. It can be used to determine a functional relationship between measured input and output data. Usually, the functional relationship is better than that obtained using regression methods. Usually, a neural network consists of an input layer, one or more hidden layers and an output layer [51]. The number of the neurons in the input layer is equal to the number of the independent variables in the experiment plus one. The extra neuron is called the bias; it has a value of one. The number of the hidden layers and the number of the neurons in each layer is chosen to provide a minimum value for the error between the measured output and the network's output while maintaining the ability of the network to generalize. In this work, we use a feed-forward, back propagation neural network with one input layer, two hidden layers, and one output layer was designed to predict the punching load. The two hidden layers have 50 and 10 neurons, respectively. The TRAINLM training function available in MATLAB neural toolbox was used to train the network using the LERNGDM adaption learning function. The input data was divided into three sets. The first set consists of 60% of the data is used to train the network. The second and third sets, each consists of 20% of the data are used to validate and test the generalization ability of the network, respectively. The sets are taken randomly out of the data set. Each hidden layer has a bias neuron as shown in Fig. 1. Several architectures were tried and the one that gave the least error was chosen. Adding more neurons increases the training time, limits the ability of the network to generalize and does not improve the results. All the

Table A.3
Slab-column connections with circular/square columns under symmetrical punching.

ID	Col. type	h, mm	C, mm	d, mm	ρ%	V_{test}, kN	f'_c, MPa	f_y, MPa	V_{test}/V_{code}						Ref.
									ACI 318-08	CEB-FIP-90	BS8110-97	EC 2 (2004)	Eq. (8)	Eq. (9)	
1	S	120	125	100	0.80	216	35.7	706	1.22	1.00	0.94	1.13	1.10	0.99	[32]
3	S	119	125	99	0.81	194	28.6	701	1.24	0.98	0.91	1.11	1.09	0.97	
5	S	220	250	200	0.80	603	30.3	657	0.92	0.88	0.83	0.83	0.89	0.87	
6	S	219	250	199	0.80	600	28.6	670	0.95	0.90	0.85	0.85	0.91	0.89	
13	S	118	125	98	0.35	145	33.3	720	0.87	0.93	0.87	1.06	1.07	0.98	
14	S	119	125	99	0.34	148	31.4	712	0.90	0.96	0.90	1.09	1.11	1.02	
17	S	220	250	200	0.34	489	31.7	668	0.73	0.93	0.88	0.88	0.97	0.98	
18	S	217	250	197	0.35	444	30.2	664	0.70	0.87	0.82	0.83	0.91	0.92	
SS2	S	100	200	77	1.2	176	23.3	500	1.30	0.99	0.92	1.20	0.94	0.98	[34]
SS4	S	100	200	77	0.92	194	33.4	500	1.19	1.05	0.98	1.28	0.99	1.06	
SS6	S	100	200	79	0.75	165	21.7	480	1.22	1.07	1.00	1.29	1.05	1.10	
SS7	S	100	200	79	0.8	186	31.2	480	1.14	1.05	0.97	1.26	1.00	1.06	
SS8	S	250	250	200	0.98	825	36.3	530	1.15	1.06	1.00	1.00	1.04	1.03	
SS9	S	160	160	128	0.98	390	34.5	485	1.36	1.11	1.05	1.18	1.17	1.08	
SS10	S	160	160	128	0.98	365	35.7	485	1.26	1.03	0.97	1.09	1.08	1.00	
SS11	S	80	80	64	0.98	117	34.5	480	1.64	1.12	1.02	1.41	1.31	1.09	
SS12	S	80	80	64	0.98	105	35.7	480	1.44	1.00	0.91	1.25	1.16	0.97	
SS13	S	80	80	64	0.98	105	37.8	480	1.40	0.98	0.89	1.23	1.13	0.95	
1	S	52	100	41	0.42	36	31.5	530	0.84	0.80	0.71	1.14	0.87	0.85	[35]
2	S	52	100	41	0.56	49	31.5	530	1.14	0.99	0.88	1.41	1.07	1.03	
3	S	52	100	41	0.69	57	31.5	530	1.33	1.08	0.95	1.53	1.15	1.10	
4	S	52	100	41	0.82	56	36.2	530	1.22	0.95	0.84	1.35	1.00	0.96	
5	S	52	100	41	0.88	57	36.2	530	1.24	0.95	0.84	1.35	0.99	0.95	
6	S	52	100	41	1.03	66	36.2	530	1.44	1.04	0.92	1.48	1.08	1.03	
7	S	52	100	41	1.16	71	30.4	530	1.69	1.14	1.01	1.62	1.19	1.12	
8	S	52	100	41	1.29	71	30.4	530	1.69	1.10	0.98	1.57	1.15	1.08	
9	S	52	100	41	1.45	79	30.4	530	1.88	1.18	1.05	1.68	1.22	1.14	
10	S	52	100	41	0.52	44	30.6	530	1.04	0.92	0.81	1.31	1.00	0.96	
11	S	52	100	41	0.8	55	30.6	530	1.30	1.00	0.88	1.42	1.06	1.01	
12	S	52	100	41	1.11	67	30.6	530	1.59	1.09	0.97	1.55	1.14	1.08	
13	S	52	100	41	0.6	49	35.3	530	1.08	0.93	0.83	1.32	0.99	0.96	
14	S	52	100	41	0.69	52	35.3	530	1.15	0.95	0.84	1.34	1.00	0.97	
15	S	52	100	41	1.99	85	35.3	530	1.87	1.09	0.96	1.55	1.10	1.03	
1A	S	58	100	47	0.44	45	29.4	530	0.91	0.84	0.75	1.15	0.94	0.89	
2A	S	58	100	47	0.69	66	29.4	530	1.33	1.07	0.95	1.46	1.16	1.08	
3A	S	58	100	47	1.29	90	29.4	530	1.82	1.18	1.06	1.62	1.25	1.14	
4A	S	58	100	47	1.99	97	31.7	530	1.89	1.08	0.96	1.47	1.11	1.01	
IB	S	46	100	35	0.42	29	39.6	530	0.74	0.73	0.64	1.08	0.77	0.79	
2B	S	46	100	35	0.69	38	39.6	530	0.97	0.82	0.71	1.21	0.84	0.84	
3B	S	46	100	35	1.29	57	39.6	530	1.45	1.00	0.87	1.47	0.99	0.98	
4B	S	46	100	35	1.99	73	31.7	530	2.08	1.19	1.04	1.76	1.18	1.14	
1C	S	65	100	54	0.42	63	28.3	530	1.08	1.01	0.91	1.33	1.14	1.05	
2C	S	65	100	54	0.69	88	33.5	530	1.39	1.13	1.02	1.49	1.24	1.14	
3C	S	65	100	54	1.29	124	33.5	530	1.95	1.29	1.17	1.71	1.38	1.24	
4C	S	65	100	54	1.99	126	28.3	530	2.16	1.20	1.09	1.59	1.27	1.12	

parameters that may affect the punching load were considered. These parameters include the concrete's strength, column size, slab depth, flexure reinforcement ratio, and the yield strength of the steel reinforcement. There is no single design code that considers all these parameters. Fig. 2 shows the relationship between the experimental data and the training, validation and testing sets. It can be shown that the relationship between the complete set of the experimental data and the data predicted by the neural network is excellent. Fig. 3 shows a comparison between the measured punching load and the punching load predicted by the neural network. Fig. 4 shows a linear regression between the experimental and the neural punching loads. The agreement is excellent as attested to by the R-value of the regression analysis.

7. Proposed equations for punching shear strength

The following equations for the prediction of punching shear strength of concrete were obtained using the regression analysis of experimental data available in the literature. For the first equation, the critical cross-section is assumed to consist of a rectangle whose edges are drawn at a distance of $0.5d$ from the column face. There is no need to identify a critical section to be used with the second equation, since the column size is used as parameter in the equation. The equations are as follows:

Equation a

$$P = v_c A_o \quad \text{kN}$$
$$A_o = 4\,(C + d)\,d \quad \text{mm}^2$$
$$v_c = 0.51(10^{-3}) f_c^{0.41} \rho^{0.38} (250/d)^{0.10} \quad \text{kN/mm}^2 \tag{8}$$

where P is the punching load (kN), v_c is the punching shear strength (kN/mm^2), A_o is the critical punching area (mm^2), C is the column size (mm), f_c is the concrete's strength (MPa), ρ is the flexure steel reinforcement ratio (%), d is the slab's depth, mm, and $k = (250/d)^{0.10}$ is the size factor of the effective depth; The value of 250 is a reflection of the measured characteristic length for high strength concrete of 70 MPa. In an earlier investigation by Marzouk and Chen [48], the characteristic length was estimated

Table A.4
Slab-column connections with circular/square columns under symmetrical punching.

ID	Col. type	h, mm	C, mm	d, mm	ρ%	V_{test}, kN	f'_c, MPa	f_y, MPa	V_{test}/V_{code}						Ref.
									ACI 318-08	CEB-FIP-90	BS8110-97	EC 2 (2004)	Eq. (8)	Eq. (9)	
S1.1	C	120	125	100	0.80	216	28.6	706	1.36	1.08	1.01	1.22	1.21	1.07	[36]
S1.2	C	119	125	99	0.81	194	22.9	701	1.38	1.05	0.98	1.19	1.20	1.05	
S2.1	C	220	250	200	0.80	603	24.2	657	1.03	0.95	0.90	0.90	0.97	0.94	
S2.2	C	219	250	199	0.80	600	22.9	670	1.06	0.97	0.92	0.92	0.99	0.96	
S1.3	C	118	125	98	0.35	145	26.6	720	0.97	1.00	0.94	1.14	1.17	1.06	
S1.4	C	119	125	99	0.34	148	25.1	712	1.01	1.04	0.97	1.17	1.22	1.10	
S2.3	C	220	250	200	0.34	489	25.4	668	0.82	1.00	0.95	0.95	1.06	1.06	
S2.4	C	217	250	197	0.35	444	24.2	664	0.78	0.94	0.89	0.89	0.99	0.99	
8	S	101	102	76	2.05	129	24.1	430	1.47	0.79	0.73	0.96	0.88	0.73	[26]
9	S	101	102	76	2.05	136	22.6	430	1.60	0.85	0.78	1.03	0.95	0.79	
10	S	101	102	76	2.05	129	24.6	430	1.46	0.79	0.72	0.95	0.87	0.73	
11	S	152	152	113	2.14	311	22.6	430	1.66	0.96	0.90	1.05	1.01	0.88	
12	S	152	203	113	2.14	357	24.8	430	1.52	0.97	0.91	1.06	0.93	0.90	
13	S	153	203	122	0.66	271	24.8	430	1.04	0.97	0.92	1.05	1.00	0.98	
14	S	102	152	73	5.01	202	25.0	430	1.86	0.84	0.77	1.02	0.79	0.73	
15	S	102	152	81	1.47	160	25.0	430	1.28	0.86	0.80	1.03	0.88	0.82	
16	S	102	152	86	0.45	107	23.2	430	0.82	0.80	0.75	0.94	0.88	0.84	
17	S	102	102	81	1.47	121	25.5	430	1.22	0.74	0.68	0.88	0.84	0.70	
19	S	152	203	123	0.47	271	22.1	430	1.09	1.12	1.05	1.20	1.18	1.16	
20	S	152	203	113	2.14	278	15.1	430	1.52	0.89	0.83	0.97	0.89	0.83	
21	S	153	203	122	0.66	230	16.1	430	1.10	0.95	0.90	1.02	1.01	0.97	
23	S	102	152	81	1.47	108	14.5	430	1.14	0.70	0.65	0.83	0.74	0.67	
25	S	153	203	122	0.66	306	52.1	430	0.81	0.86	0.81	0.92	0.83	0.86	
26	S	102	203	73	5.01	323	52.1	430	1.68	0.92	0.85	1.13	0.77	0.82	
27	S	102	152	81	1.47	243	52.1	430	1.35	1.03	0.95	1.22	0.99	0.97	
28	S	102	152	86	0.45	148	52.1	430	0.76	0.85	0.79	1.00	0.87	0.88	

to have an average value of 500 mm and 250 mm for normal and high-strength concrete, respectively.

Equation b

$$P = 12.30\,(c+d)^{0.53} f_c^{0.34} \rho^{0.41} (d/250)^{1.22} \quad \text{kN/mm}^2 \tag{9}$$

where P is the punching load (kN), c is the column size (mm), $\grave{f}_c$ is the concrete strength (MPa), ρ is the flexure steel ratio (%), and d is the concrete depth (mm).

8. Statistical verification of the proposed equations

Eqs. (8) and (9) have been validated using the existing experimental data. Figs. 5 and 6 show a comparison between the values of the punching load obtained using Eqs. (8) and (9) and those obtained from the experimental results. The figures show that there is an excellent agreement between the proposed equations and the test results (244 slabs).

9. Comparison between neural network output, proposed equations and design codes

Table 1 provides the mean value, the standard deviation, the coefficient of variation, and the confidence intervals of the means for the ratios of V_{Test}/V_{neural}, $V_{Test}/V_{eq.}$ and the ratio for the test load and the load estimated by equations in different well-known specifications. V_{Test}/V_{neural} is the ratio of the experimental punching load to the punching load obtained by neural network. The mean value provided by BS 8110-97 is near unity, where the mean value provided by CEB-FIP-90 is 0.95. This means that the estimated values are close to experimental values. The coefficients of variation in BS8110-97 and CEB-FIP-90 are 13%. The coefficient of variation of CSA-A23.3-04 and ACI 318-08 is 27%. In some cases the ACI 318-08 underestimated the punching shear values by more than 50% and in some cases the ACI 318-08 equation overestimated the punching shear value by more than 50%. For example, in the case of specimens PG-2b and PG-4 tested by Guandalini and Muttoni [43], which were made of normal strength concrete with an effective depth of 210 mm and small reinforcement ratio of 0.25%, the ACI 318-08 code overestimated the punching shear capacity by more than 100%; also in case of specimen HSC9 tested by Hallgren [40], which were made of high strength concrete with an effective depth of 200 mm and small reinforcement ratio of 0.33%, the ACI 318-08 code overestimated the punching shear capacity by more than 100%, and this is due to neglecting the size effect factor as well as the effect of reinforcement ratio.

The mean, the standard deviation and the coefficient of variation of the proposed equations obtained from Equations a and b are given in Table 1. The mean of $V_{Test}/V_{eq.}$, is 1.00, and coefficient of variation is 15% and 12% for the analyzed database. These coefficients of variation are small in spite of the simplicity of the equations.

The standard errors and the 95% confidence intervals are shown also in Table 1. It can be noticed that the proposed Eq. (9) has a standard error of 0.015 while the CSA, ACI have a standard error of 0.043 and 0.036, respectively. The CEB and BS8110 have the same standard error of 0.016 while the EC 2 has 0.026. The proposed Eq. (9) has better estimated of punching load of slabs than all the available equations from the point of view of statistics and probability.

The evaluated values for the ACI 318-08, CSA-A23.3-04, BS 8110-97, CEB-FIB 90 and EC2 (2004) versus test results are shown in Figs. 7–11. The figures show a scatter of the values calculated using ACI 318-08 and CSA-A23.3-04 equations. On the other hand, the equations suggested in the present paper have a small coefficient of variation and better confidence intervals.

10. Conclusions

This paper provides the designer with a reliable design tool for estimating the punching shear strength of two way slabs. Two approaches are presented; the first was the neural networks

Table A.5
Slab-column connections with circular/square columns under symmetrical punching.

ID	Col. type	h, mm	C, mm	d, mm	ρ%	V_{test}, kN	f'_c, MPa	f_y, MPa	V_{test}/V_{code}						Ref.
									ACI 318-08	CEB-FIP-90	BS8110-97	EC 2 (2004)	Eq. (8)	Eq. (9)	
NS1	S	120	150	95	1.47	320	42.0	490	1.61	1.17	1.09	1.34	1.17	1.10	
HS1	S	120	150	95	0.49	178	67.0	490	0.71	0.80	0.75	0.92	0.81	0.82	
HS2	S	120	150	95	0.84	249	70.0	490	0.97	0.92	0.86	1.06	0.91	0.91	
HS7	S	120	150	95	1.19	356	74.0	490	1.35	1.16	1.08	1.32	1.12	1.10	
HS3	S	120	150	95	1.47	356	69.0	490	1.39	1.10	1.03	1.26	1.06	1.04	
HS4	S	120	150	90	2.37	418	66.0	490	1.80	1.21	1.13	1.41	1.14	1.10	
NS2	S	150	150	120	0.94	396	30.0	490	1.69	1.34	1.26	1.44	1.44	1.31	
HS5	S	150	150	125	0.64	365	68.0	490	0.98	1.01	0.95	1.08	1.05	1.01	
HS6	S	150	150	120	0.94	489	70.0	490	1.37	1.25	1.18	1.35	1.26	1.21	[25]
HS8	S	150	150	120	1.11	436	69.0	490	1.23	1.06	1.00	1.14	1.07	1.02	
HS9	S	150	150	120	1.61	543	74.0	490	1.48	1.14	1.08	1.23	1.12	1.07	
HS10	S	150	150	120	2.33	645	80.0	490	1.69	1.17	1.10	1.26	1.12	1.06	
HS11	S	90	150	70	0.95	196	70.0	490	1.15	1.06	0.98	1.32	1.00	1.04	
HS12	S	90	150	70	1.52	258	75.0	490	1.47	1.17	1.08	1.45	1.08	1.11	
HS13	S	90	150	70	1.87	267	68.0	490	1.59	1.17	1.08	1.45	1.07	1.09	
HS14	S	120	220	95	1.47	498	72.0	490	1.49	1.31	1.23	1.51	1.14	1.25	
HS15	S	120	300	95	1.47	560	71.0	490	1.34	1.28	1.20	1.47	1.02	1.26	
65-1-1	S	300	200	275	1.49	2050	64.0	500	1.49	1.24	1.17	1.17	1.25	1.18	
95-1-1	S	300	200	275	1.49	2250	84.0	500	1.42	1.25	1.17	1.17	1.23	1.18	
115-1-1	S	300	200	275	1.49	2450	112.0	500	1.34	1.23	1.16	1.16	1.19	1.16	
95-1-3	S	300	200	275	2.55	2400	90.0	500	1.47	1.09	1.02	1.02	1.04	0.99	
65-2-1	S	225	150	200	1.75	1200	70.0	500	1.55	1.16	1.10	1.10	1.20	1.09	
95-2-1D	S	225	150	200	1.75	1100	88.0	500	1.27	0.99	0.93	0.93	1.00	0.92	
95-2-1	S	225	150	200	1.75	1300	87.0	500	1.51	1.17	1.10	1.10	1.19	1.09	[38]
115-2-1	S	225	150	200	1.75	1400	119.0	500	1.39	1.14	1.07	1.07	1.13	1.06	
95-2-3	S	225	150	200	2.62	1450	90.0	500	1.65	1.13	1.07	1.07	1.12	1.02	
95-2-3D	S	225	150	200	2.62	1250	80.0	500	1.51	1.01	0.96	0.96	1.02	0.92	
95-2-3D+	S	225	150	200	2.62	1450	98.0	500	1.59	1.10	1.04	1.04	1.09	0.99	
115-2-3	S	225	150	200	2.62	1550	108.0	500	1.61	1.14	1.07	1.07	1.12	1.03	
95-3-1	S	113	100	88	1.84	330	85.0	500	1.64	1.12	1.04	1.31	1.16	1.04	
HSC0	S	225	250	200	0.80	965	90.0	643	0.86	0.98	0.93	0.93	0.91	0.96	
HSC1	S	225	250	200	0.80	1021	91.0	627	0.90	1.03	0.98	0.98	0.96	1.02	
HSC2	S	225	250	194	0.82	889	86.0	620	0.84	0.95	0.90	0.91	0.88	0.93	
HSC4	S	225	250	200	1.19	1041	92.0	596	0.91	0.92	0.87	0.87	0.84	0.88	[40]
HSC6	S	225	250	201	0.60	960	109.0	633	0.77	1.00	0.95	0.95	0.93	1.00	
HSC9	S	225	250	202	0.33	565	84.0	634	0.51	0.78	0.74	0.73	0.75	0.82	
N/HSC8	S	225	250	198	0.80	944	95.0	631	0.83	0.96	0.91	0.91	0.88	0.94	

approach and the second was the regression approach. A database of 244 tests available in the literature and conducted by the authors was used to train the neural network and to calculate the parameters of two practical equations for shear strength of two way slabs. The database has a wide range of slab thicknesses (35–500 mm) and reinforcement ratios (0.25%–5.00%). Neural networks were applied to predict the punching strength of two-way slabs. The two hundred and forty four test specimens from the punching shear database were used for training and testing the proposed model (60% of the data for training, 20% of the data for validation and 20% of the data for testing). The validation and testing data sets were not used in the training process.

New alternative design equations are proposed. The new equations can accurately predict the punching shear strength of interior slab–column connections without shear reinforcement. This study showed that concrete compressive strength, slab thickness, column size and flexure reinforcement ratio are the primary parameters that dominate the punching behavior of slab–column connections. The ACI 318-08 equation ignores the reinforcement ratio and the slab's depth. The analysis of the available database supports the fact that the punching strength increases as the reinforcement ratio increases. Two simplified practical punching strength equations are proposed from the analysis of the present database. The coefficients of variation and the standard error of the punching strength ratio evaluated from the equations are smaller than that yielded by the ACI 318-08 equation. The mean of punching strength is 1.00 for both equations, and the coefficients of variation are 15% and 12%, respectively for the analyzed database. The standard errors at 95% confidence interval of the proposed equations are 0.019 and 0.015, respectively. The Eq. (9) proposed in this work yielded better results than all available design codes equations as it includes all the effective variables that affect the punching shear in spite of still being a simple equation. The collected data base helped in yielding better equations that can provide better estimates of the punching loads, wider applicability range, and better statistical results. The developed equations are intended to be used by design engineers.

Acknowledgements

The authors are grateful to the Natural Sciences and Engineering Research Council of Canada (NSERC) for providing the funds for the project.

Appendix. Experimental data

Tables A.1–A.7 of the Appendix list the data used to obtain the results of this paper. This data is available in the open literature. Tables A.1–A.7 show the details of the data as well as the references from where it was obtained.

Table A.6
Slab-column connections with circular/square columns under symmetrical punching.

ID	Col. type	h, mm	C, mm	d, mm	ρ%	V_{test}, kN	f'_c, MPa	f_y, MPa	V_{test}/V_{code}						Ref.
									ACI 318-08	CEB-FIP-90	BS8110-97	EC 2 (2004)	Eq. (8)	Eq. (9)	
1	S	125	150	98	0.58	224	88.2	550	0.74	0.83	0.78	0.95	0.83	0.84	
2	S	125	150	98	0.58	212	56.2	550	0.88	0.92	0.86	1.04	0.94	0.93	
3	S	125	150	98	0.58	169	26.9	550	1.02	0.93	0.87	1.06	1.01	0.95	
4	S	125	150	98	0.58	233	58.7	550	0.95	0.99	0.93	1.13	1.01	1.00	
6	S	125	150	98	0.58	233	101.8	550	0.72	0.83	0.77	0.94	0.81	0.83	
12	S	125	150	98	1.28	319	60.4	550	1.28	1.04	0.97	1.18	1.02	0.99	
13	S	125	150	98	1.28	297	43.4	550	1.40	1.08	1.01	1.22	1.08	1.03	
14	S	125	150	98	1.28	341	60.8	550	1.36	1.11	1.03	1.25	1.09	1.05	[39]
16	S	125	150	98	1.28	362	98.4	550	1.14	1.00	0.94	1.14	0.95	0.95	
21	S	125	150	98	1.28	286	41.9	650	1.38	1.05	0.98	1.19	1.06	1.00	
22	S	125	150	98	1.28	405	84.2	650	1.38	1.18	1.10	1.34	1.13	1.12	
23	S	125	150	100	0.87	341	56.4	650	1.38	1.25	1.17	1.41	1.26	1.23	
25	S	125	150	100	1.27	244	32.9	650	1.29	0.94	0.88	1.07	0.97	0.90	
26	S	125	150	100	1.27	294	37.6	650	1.45	1.09	1.02	1.23	1.11	1.04	
27	S	125	150	102	1.03	227	33.7	650	1.15	0.91	0.85	1.02	0.95	0.88	
P100	S	135	200	100	0.97	330	39.4	488	1.33	1.18	1.11	1.34	1.13	1.16	
P150	S	190	200	150	0.90	583	39.4	465	1.34	1.22	1.15	1.24	1.22	1.19	
P200	S	240	200	200	0.83	904	39.4	465	1.36	1.27	1.20	1.20	1.32	1.25	
P300	S	345	200	300	0.76	1381	39.4	468	1.11	1.07	1.00	1.00	1.16	1.08	[42]
P400	S	450	300	400	0.76	2224	39.4	433	0.96	1.02	0.95	0.95	1.03	1.02	
P500	S	550	300	500	0.76	2681	39.4	433	0.81	0.87	0.79	0.79	0.89	0.87	
PG-1	S	250	260	210	1.50	1024	27.6	400	1.50	1.15	1.09	1.09	1.13	1.09	
PG-2	S	250	260	210	0.25	445	28.5	400	0.64	0.89	0.85	0.85	0.95	0.97	
PG-2b	S	250	260	210	0.25	439	40.5	400	0.53	0.78	0.74	0.74	0.81	0.85	
PG-3	S	504	520	464	0.33	2153	32.4	400	0.63	0.97	0.90	0.90	0.92	1.03	
PG-4	S	250	260	210	0.25	408	32.2	400	0.55	0.79	0.75	0.75	0.83	0.85	
PG-5	S	250	260	210	0.33	550	29.3	400	0.78	1.00	0.95	0.95	1.05	1.06	[43]
PG-6	S	136	130	96	1.50	236	34.7	400	1.40	0.94	0.88	1.07	0.99	0.89	
PG-7	S	140	130	100	0.75	243	34.7	400	1.36	1.15	1.07	1.29	1.26	1.14	
PG-8	S	142	130	102	0.33	141	34.7	400	0.77	0.85	0.80	0.96	0.97	0.90	
PG-9	S	142	130	102	0.25	118	34.7	400	0.64	0.78	0.73	0.87	0.90	0.84	
PG-10	S	250	260	210	0.33	540	28.5	400	0.78	0.99	0.94	0.94	1.04	1.05	

Table A.7
Slab-column connections with circular/square columns under symmetrical punching.

ID	Col. type	h, mm	C, mm	d, mm	ρ%	V_{test}, kN	f'_c, MPa	f_y, MPa	V_{test}/V_{code}						Ref.
									ACI 318-08	CEB-FIP-90	BS8110-97	EC 2 (2004)	Eq. (8)	Eq. (9)	
C1	S	120	250	100	0.80	270	24.0	718	1.19	1.10	1.04	1.25	1.04	1.12	
C2	S	120	250	100	0.80	250	24.4	718	1.10	1.02	0.96	1.15	0.96	1.03	[44]
D1	S	145	150	125	0.64	265	27.2	718	1.12	0.99	0.93	1.06	1.10	1.00	
1	S	160	250	124	1.54	483	33.1	488	1.37	1.08	1.02	1.16	0.99	1.03	
7	S	230	300	190	1.30	825	33.5	531	1.16	1.01	0.96	0.97	0.93	0.96	[45]
10	S	300	350	260	1.10	1046	31.0	524	0.90	0.84	0.80	0.80	0.79	0.81	
NSC1	S	200	250	158	2.17	678	35.0	490	1.35	0.95	0.90	0.96	0.88	0.88	
HSC1	S	200	250	138	2.48	788	68.5	490	1.35	1.03	0.97	1.07	0.88	0.93	
HSC2	S	200	250	128	2.68	801	70.0	490	1.51	1.12	1.06	1.19	0.95	1.01	
HSC3	S	200	250	158	1.67	802	66.7	490	1.16	0.99	0.94	1.00	0.88	0.93	
HSC4	S	200	250	158	1.13	811	61.2	490	1.22	1.18	1.12	1.19	1.07	1.13	[46]
HSC5	S	150	250	113	1.88	480	70.0	490	1.07	0.89	0.84	0.98	0.76	0.83	
NSC2	S	200	250	163	0.52	479	33.0	490	0.94	1.05	1.00	1.05	1.05	1.08	
NSC3	S	150	250	105	0.40	228	34.0	490	0.79	0.98	0.92	1.10	0.94	1.04	
NS1	S	150	250	105	0.45	219	44.7	400	0.67	0.83	0.78	0.93	0.77	0.87	
NS2	S	200	250	153	0.55	491	50.2	400	0.86	1.01	0.96	1.02	0.96	1.03	
NS3	S	250	250	183	0.35	438	35.0	400	0.71	0.92	0.87	0.89	0.94	0.97	
HS1	S	250	250	183	0.35	574	70.0	400	0.66	0.95	0.91	0.93	0.93	1.00	
NS4	S	300	250	218	0.73	882	40.0	400	1.04	1.07	1.01	1.01	1.07	1.07	
HS2	S	300	250	218	0.73	1023	64.7	400	0.95	1.06	1.00	1.00	1.02	1.05	[52]
HS3	S	300	250	220	0.43	886	76.0	400	0.74	1.02	0.96	0.96	0.99	1.05	
HS4	S	350	400	268	1.13	1721	75.0	400	0.84	0.94	0.89	0.89	0.80	0.90	
HS6	S	350	400	263	1.44	2090	65.4	400	1.13	1.14	1.08	1.08	0.96	1.07	
NS4	S	400	400	313	1.57	2234	40.0	400	1.20	1.08	1.02	1.02	0.96	1.02	
HS7	S	400	400	313	1.57	2513	60.0	400	1.10	1.06	1.00	1.00	0.92	1.00	

References

[1] American Concrete Institute (ACI). Building code requirements for structural concrete. ACI 318-08. Farmington Hills, Michigan; 2008.
[2] Canadian Standards Association (CSA). Design of concrete structures for buildings. CSA-A23.3-04. Rexdale, Ontario, Canada; 2004.
[3] British Standards Association BS 8110-85. Structural use of concrete. Use of concrete. Part 1: Code of Practice for Design and Construction. BSI. Milton Keynes, BS 8110; 1985.
[4] Comité Euro–International Du Béton–Fédération de la Précontrainte (CEB–FIP). Model Code. Bulletin D'Information No. 203–305. Lausanne, Switzerland; 1990.
[5] European Committee for Standardization Eurocode 2 (CEN). Design of concrete structures-Part 1.1: general rules and rules for buildings. Brussels, Belgium; 2004. 225 pp.
[6] Bhatt P, Agar TJA. A neural network for predicting the punching shear strength of internal column-flat slab junctions without shear reinforcement. In: International workshop on punching shear capacity of RC slabs. 2000. 57, p. 39–46.
[7] Dias WPS, Pooliyadda SP. Neural networks for predicting properties of concretes with admixtures. Construct Build Mater 2001;15:371–9.
[8] Lee S. Prediction of concrete strength using artificial neural networks. Eng Struct 2003;25:849–57.
[9] Kawamura K, Miyamoto A, Frangopol DM, Kimura R. Performance evaluation of concrete slabs of existing bridges using neural networks. Eng Struct 2003; 25:1455–77.
[10] Alqedra MA, Ashour AF. Prediction of shear capacity of single anchors located near a concrete edge using neural networks. Comput Struct 2005;83: 2495–502.
[11] Hoła J, Schabowicz K. New technique of nondestructive assessment of concrete strength using artificial intelligence. NDT&E International 2005;38:251–9.
[12] Ahmadkhanlou F, Adeli H. Optimum cost design of reinforced concrete slabs using neural dynamics model. Eng Appl Artif Intell 2005;18(1):65–72.
[13] Ji T, Lin T, Lin X. A concrete mix proportion design algorithm based on artificial neural networks. Cement Concr Res 2006;36:1399–408.
[14] Öztaş A, Pala M, Özbay E, Kanca E, Çağlar N, Bhatti MA. Predicting the compressive strength and slump of high strength concrete using neural network. Constr Build Mater 2006;20:769–75.
[15] Choi K, Taha M, Sherif A. Simplified punching shear design method for slab–column connections using fuzzy learning. ACI Struct J 2007;104(4): 438–47.
[16] Pendharkar U, Chaudhary S, Nagpal AK. Neural network for bending moment in continuous composite beams considering cracking and time effects in concrete. Eng Struct 2007;29:2069–79.
[17] Demir F. Prediction of elastic modulus of normal and high strength concrete by artificial neural networks. Constr Build Mater 2008;22:1428–35.
[18] Caglar N, Elmas M, Yaman ZD, Saribiyik M. Neural networks in 3-dimensional dynamic analysis of reinforced concrete buildings. Constr Build Mater 2008; 22:788–800.
[19] Trtnik G, Kavčič F, Turk G. Prediction of concrete strength using ultrasonic pulse velocity and artificial neural networks. Ultrasonics 2009;49:53–60.
[20] Alshihri MM, Azmy AM, El-Bisy MS. Neural networks for predicting compressive strength of structural light weight concrete. Constr Build Mater 2009;23:2214–9.
[21] Caglar N. Neural network based approach for determining the shear strength of circular reinforced concrete columns. Constr Build Mater 2009;23:3225–32.
[22] Dahou Z, Sbartaï ZM, Castel A, Ghomari F. Artificial neural network model for steel-concrete bond prediction. Eng Struct 2009;31:1724–33.
[23] Erdem H. Prediction of the moment capacity of reinforced concrete slabs in fire using artificial neural networks. Adv Eng Software 2010;41:270–6.
[24] Lee SC, Park SK, Lee BH. Development of the approximate analytical model for stub-girder system using neural networks. Comput Struct 2001;79(10): 1013–25.
[25] Marzouk H, Hussein A. Experimental investigation on the behavior of high-strength concrete slabs. ACI Struct J 1991;88(6):701–13.
[26] Gardner N. Relationship of the punching shear capacity of reinforced concrete slabs with concrete strength. ACI Struct J 1990;87(1):66–71.
[27] Elstner R, Hognestad E. Shearing strength of reinforced concrete slabs. ACI J Proc 1956;53(1):29–58.
[28] Kinnunen S, Nylander H. Punching of concrete slabs without shear reinforcement. Transactions No. 158. Royal Institute of Technology. Stockholm, Sweden; 1960. 112 pp.
[29] Moe J. Shearing strength of reinforced concrete slabs and footings under concentrated loads. Development Department Bulletin No. D47. Portland Cement Association. Skokie; 1961. 130 pp.
[30] Yitzhaki D. Punching strength of reinforced concrete slabs. ACI J Proc 1966; 63(5):527–40.
[31] Mowrer R, Vanderbilt M. Shear strength of lightweight aggregate reinforced concrete flat plates. ACI J Proc 1967;64(11):722–9.
[32] Kinnunen S, Nylander H, Tolf P. Investigations on punching at the division of building statics and structural engineering. Nordisk Betong. Stockholm 1978; 3:25–7.
[33] Magura D, Corley W. Tests to destruction of a multipanel waffle slab structure. Full-Scale Testing of New York World's Fair Structures. Publication 1721. Building Research Advisory Board. National Academy of Sciences. Washington DC, II; 1969. p. 10–135.
[34] Regan P, Walker P, Zakaria K. Tests of reinforced concrete flat slabs. CIRIA Project No. RP 220. Polytechnic of Central London; 1979.
[35] Rankin G, Long A. Predicting the punching strength of conventional slab–column specimens. Proc Instit Civ Eng, Part 1 1987;82:327–46.
[36] Tolf P. Plattjocklekens inverkan pøa betongplattors høallfasthet vid genomstansning Försök med cirkulära platter. Bulletin No. 146. Department of Structural Mechanics and Engineering. Royal Institute of Technology. Stockholm, 64 pp. (in Swedish with summary in English); 1988.
[37] Mongai G. A critical review of the symmetric punching shear of reinforced concrete flat slabs. Master's thesis. University of Ottawa; 1990. 252 pp.
[38] Tomaszewicz A. Punching shear capacity of reinforced concrete slabs. High Strength Concrete SP2-Plates and Shells. Report 2.3. Report No. STF70A93082. SINTEF. Trondheim; 1993. 36 pp.
[39] Ramdane K. Punching shear of high performance concrete slabs. In: Proceedings of the 4th international symposium on utilization of high strength high performance concrete. Paris; 1996. p. 1015–26.
[40] Hallgren M. Punching shear capacity of reinforced high strength concrete slabs. Bulletin 23, Department of Structural Engineering. Royal Institute of Technology. Stockholm; 1996. 206 pp.
[41] Marzouk H, Jiang D. Experimental investigation on shear enhancement types for high-strength concrete plates. ACI Struct J 1997;94(1):49–58.
[42] Kevin K. Influence of size on punching shear strength of concrete slabs. Master's thesis. McGill University. Montreal; 2000. 92 pp.
[43] Guandalini S, Muttoni A. Symmetrical punching tests on slabs without transverse reinforcement. Test Report. École Polytechnique Fédérale de Lausanne. Lausanne. Switzerland; 2004. 85 pp.
[44] Sundquist H, Kinnunen S. The effect of column head and drop panels on the punching capacity of flat slabs. Bulletin No. 82. Department of Civil and Architectural Engineering. Royal Institute of Technology. Stockholm, 24 pp. (in Swedish with summary and Figure captions in English); 2004.
[45] Birkle G, Dilger W. Influence of slab thickness on punching shear strength. ACI Struct J 2008;105(2):180–8.
[46] Marzouk H, Hossin M. Crack analysis of reinforced concrete two-way slabs. Research Report RCS01, Faculty of Engineering and Applied Science, Memorial University of Newfoundland, St. John's, Newfoundland; 2007. 159 pp.
[47] Rizk E. Structural behaviour of thick concrete plates. Ph.D. thesis, Faculty of Engineering, Memorial University of Newfoundland, St. John's, NL, Canada; 2010.
[48] Marzouk H, Chen W. Fracture energy and tension properties of high-strength concrete. ASCE J Mater Civ Eng 1995;7(2):108–16.
[49] Marzouk H, Emam M, Hilal M. Sensitivity of shear strength to fracture energy of high-strength concrete slabs. Canad J Civ Eng 1998;25(1):40–50.
[50] Staller. Analytical studies and numerical analysis of punching shear failure in reinforced concrete slabs. FIB Bulletin on Punching of Structural Concrete Slabs dedicated to Professor Sven Kinnunen. In International Workshop on punching shear capacity of reinforced concrete slabs, Proceedings, Eds.: Silfwerbrand, J.; Hassanzadeh, G.. Kungl. Tekniska Högskolan Stockholm, TRITA-BKN. Bull. 57; 2000.
[51] Elshafey A, Haddara M, Marzouk H. Damage detection in offshore structures using neural networks. Marine Struct 2010;23(1):131–45.
[52] Marzouk, Rizk. Punching analysis of reinforced concrete two-way slabs, Research Report RCS01, Faculty of Engineering and Applied Science, Memorial University of Newfoundland, St. John's, Newfoundland, Canada; 2009. 159 pp.